ICAST2014#083

# Smart Actuation of Inlet Guide Vanes for Small Turbine Engine

Razvan Rusovici, Joshuo Feys[2], Paavo Sepri[3], Chelakara Subramanian[4]

[1] Mechanical and Aerospace Engineering, Florida Institute of Technology, Melbourne, FL, U.S.A.

## Abstract

The research focused on the conceptual design a compact smart actuation mechanism for miniature turbine inlet guide vanes (IGV) or compressor vanes. Variable inlet guide vanes (VIGV) on larger turbine engines are commonly equipped with hydraulic or electric actuators. These conventional methods, particularly hydraulically amplified actuators, do not translate easily into small scale turbojets. There is a need to develop suitable actuation mechanisms for IGV on this scale. Power efficiency and size are the largest caveats with conventional mechanisms. IGV array was designed for a small turbojet engine measuring 76.2-mm in overall diameter. The inlet guide vane would turn the inlet flow $35^0$ to $45^0$, requiring a $10^0$ adjustment range on their position. For a Mach 0.4 flow condition, the maximum moment around one blade in the array was calculated to be approximately 0.05 N*m. This moment was transferred by a crank slider mechanism to a central ring which actuated all twelve blades. Calculations were performed to determine the required actuation force and materials used in the assembly. The piezo-inchworm motor power consumption was found. The "smart" actuation system detailed in this conceptual design could be modified to fit a wide range of miniature turbines in future work.

## 1. INTRODUCTION

Unmanned, small scale fixed wing aircraft have been widely used in military and commercial applications [1]. Since smaller UAV use turbojet engines, design solutions are needed to improve the operating envelope of the small-scale jet engines. The turbojet engines designed especially for UAV or missiles are characterized by thrust on the order of hundreds of Newtons, and due to size and weight limitations, may not feature advanced flow control devices such as inlet guide vanes (IGV) [2]. The airflow entering the compressor [3] section of a turbojet is often turbulent due to the high angle of incidence between engine inlet and free-stream velocity, or because of existing atmospheric turbulence. Actuated, variable IGV (VIGV) are used to help control the relative angle of incidence of the flow that enters the engine compressor, thereby preventing flow separation, compressor stall and thus extending the compressor's operating envelope [4]. Turbine jet-engines which employ VIGV were developed by Rolls Royce (Trent DR-900) and General Electric (J79).
The aim of the current work was to present a conceptual design of a variable angle-of-attack (AOA), smart-material actuated, IGV row. The main goal was to demonstrate that a smart material actuation system would be capable of producing the required force and displacement for the VIGV row and that it would be simple and compact.

### 1.1 Literature survey of actuation devices for turbomachinery vanes

Turbomachinery vanes include both inlet guide vanes and compressor stator vanes. Wanger [5] invented an-IGV angle-of-attack (AOA) control device that used hydraulic actuation. The IGV control device consisted of a hydraulic

piston (actuator), and crank--slider mechanisms (see Figure 1). Groups of three vanes were connected via a common link and controlled by a single hydraulic actuator.

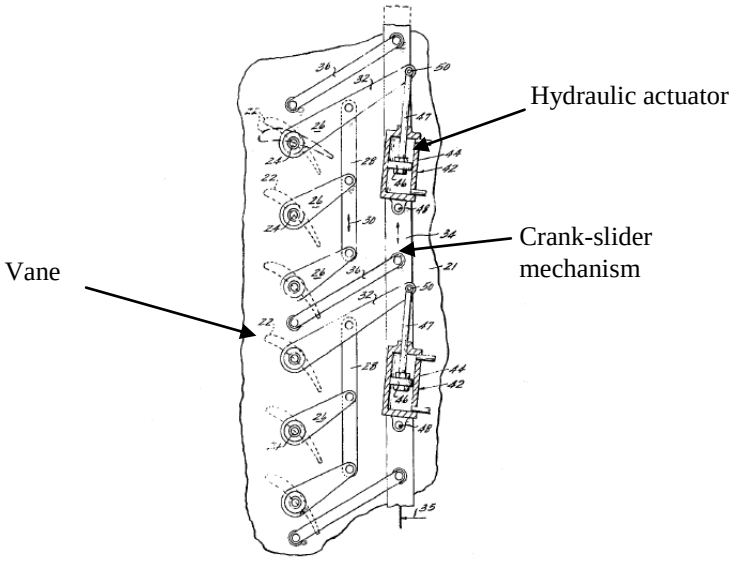


**Figure 1**Top View of IGV actuation mechanism [5]

Patel et al. [6] developed a variable-AOA, compressor stator-vanes that were independently-controlled via electric motor actuation. This allowed for superior compressor performance since it became possible to alleviate stall occurring over the axial compressor sections due to flow separation, by changing the AOA of each vane. Figure 2 shows the single pivoting stator vane [6].

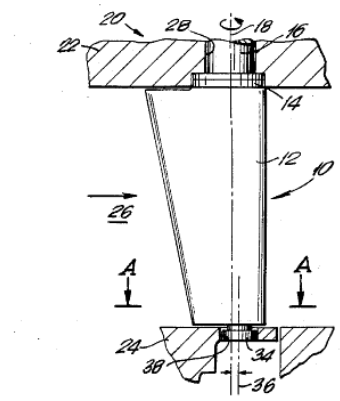


**Figure 2** Electrically-actuated stator vane [6]

### 1.2 Piezoelectric inchworm motors

Piezoelectric inchworm motors have been employed in to provide accurate (nano- or micro-scale resolution) and displacements (millimeter or centimeter scale); the displacements produced by the piezo-inchworms are significantly larger than those produced by piezoceramic stack actuators, at the expense of actuation speed. Piezo-inchworms have taken many shapes [7], [8]. The most widespread inchworm designs uses three piezoceramic stack actuators, all contained in a single casing, and relies upon a simple principle of operation (Figure 3). Stack actuators are powered in sequence in order to grip, translate and release a movable shaft. The first stack's axis axis lies

perpendicular to the longitudinal axis of the shaft and produces the aft grip. The second (extensional) stack's axis lies parallel to that of the shaft. The third stack lies perpendicular to the shaft longitudinal axis, and produces a fore grip. The fore and aft grip stacks alternatively grab and release the shaft, while the second stack alternatively expands and contracts. The inchworm moves the shaft via a six-step process: extension of the second stack; extension of the aft grip stack; relaxation of the fore grip stack; relaxation of the second stack; extension of the fore grip stack; relaxation of the aft grip stack

.

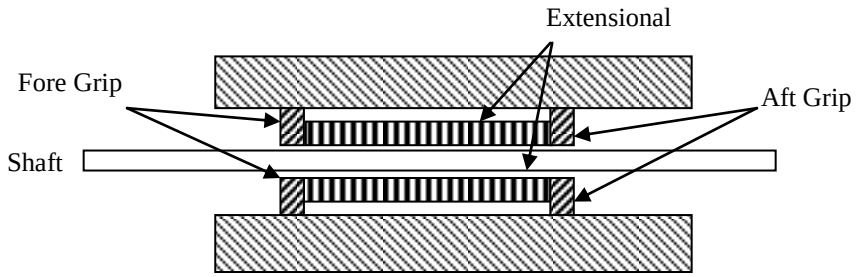


**Figure 3** Schematic of piezoelectric inchworm actuator

Such piezoelectric inchworm motors are manufactured by many companies, including Physik Instrumente™. For example, the PI™N-310 NEXACT® OEM Miniature Linear Motor/Actuator(considered in this work to provide the required force and travel) exhibits linear push/pull force of maximum 10 N, while providing a maximum of 125 mm and a minimum of 20 mm of travel with 25 nm displacement resolution. The actuator has a block shape with 25mm x25mm x 12mm dimensions. The maximum voltage required for actuation is 40. The piezoelectric inchworm actuator has the ability to be self-locking.


**Figure 4** PI™ N-310 actuator

## 2. CONCEPTUAL DESIGN

The conceptual design aimed to demonstrate the successful incorporation of smart actuators for variable IGV (VIGV) actuation. First, a target small jet engine featuring IGV was targeted. The same method described by this research may be applied to other small, or large, jet engine employing VIGV. The following set of requirements was used to prove the concept of smart-actuated VIGV. The engine casing has an outside diameter of 100 mm and produces a thrust force of 120.1 N. The conceptual design performance parameters given by the engine manufacturer (Florida Turbine Technologies) were:

- Thrust output of 120.1 N
- IGV angle of attack varies from 35 to 45 degrees and features NACA 65210 airfoil
- Inner Diameter: 30.5 mm, Outer Diameter: 76.2 mm, Solidity ratio of 1.2
- Maximum inlet Mach number: 0.4

The objective of this project was to design a variable IGV array to fit this engine that would be effective, reliable, and efficient. Using the given performance parameters, the aerodynamic forces and moments acting upon the IGVs were found via mass and momentum-continuity theory used in a control volume approach [10] applied to a cascade of blades, Figure 5.

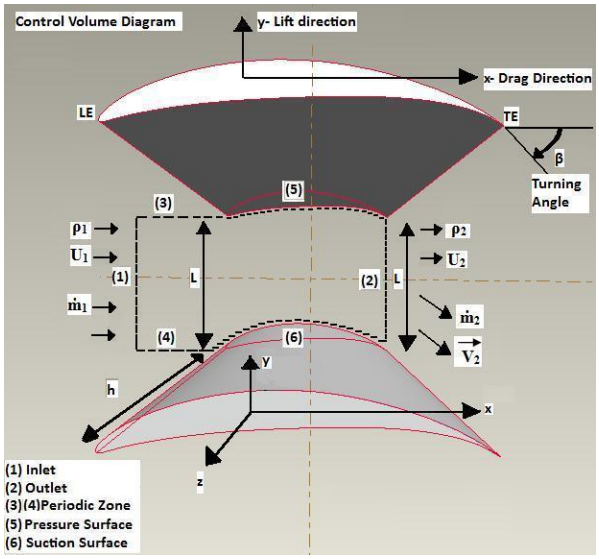


**Figure 5** Diagram of the control volume

These parameters, plotted in Figures 6-8 were used to determine the force and power requirements of the entire mechanism ($\epsilon = \frac{\delta}{L}$ is the ratio of the boundary layer to the length L between adjacent blades).

- Maximum aerodynamic moment around each IGV: 0.05 N·m
- Maximum lift force per IGV: 7.38 N
- Maximum drag force per IGV: 3.75 N

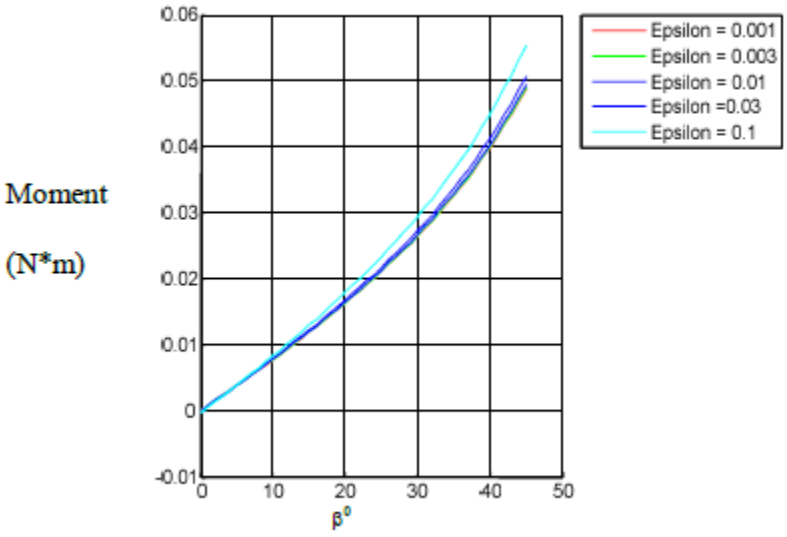


**Figure 6:** Aerodynamic moment vs turning angle

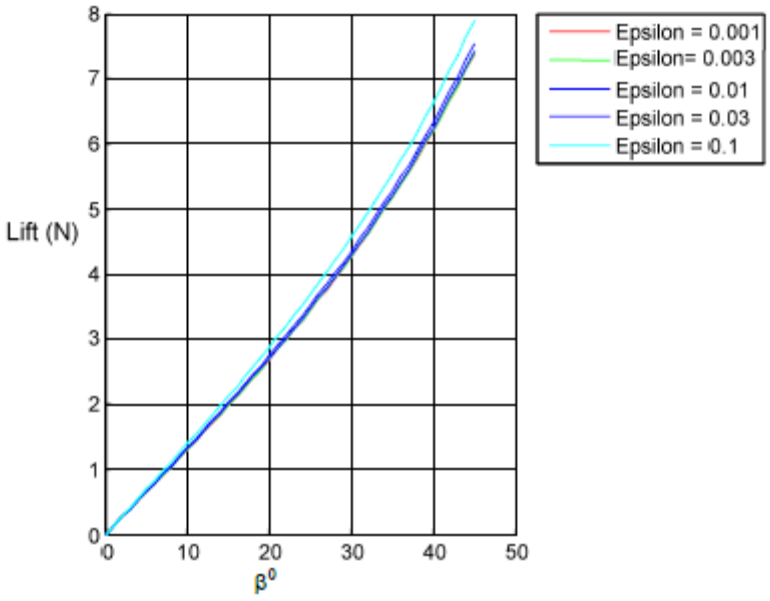


**Figure 7:** Aerodynamic lift vs turning angle

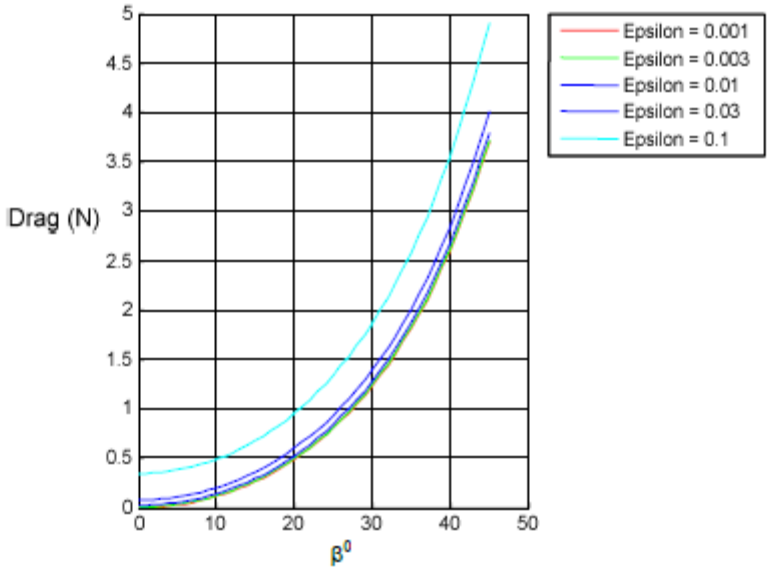


**Figure 8:** Aerodynamic drag vs turning angle

## 2.1 Proposed actuation mechanism

The mechanism proposed in this paper is an improved version of the mechanism proposed by Rusovici *et al*, 2011 [10], based on a crank-slider mechanism. Figure 9 shows the IGV array. This design incorporated the original reverse crank slider design in an annular pattern, linked to twelve individual IGVs. Each group has three pivot points, A, B, and C. The links connecting these points are each 25 mm long. Pivot A allows rotation along the axis through the IGV, while B and C allow full three-axis rotation through the use of a 5 mm ball joint. At C, the link BC is attached to a ring that slides over the compressor casing. This ring connects all IGV linkages together and allows for the array to be actuated with fewer actuators than there are guide vanes.

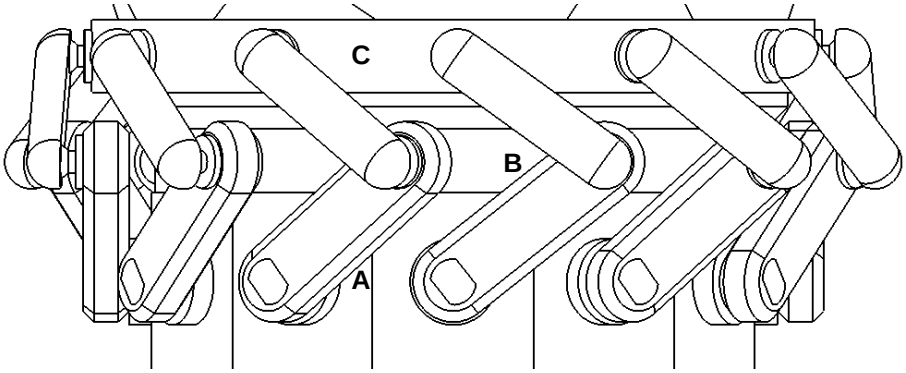


**Figure 9: Annular crank slider array, pins A, B, and C annotated**

Due to the extra degrees of freedom (DOF) gained by the use of ball joints, the ring could be translated axially, or rotated around the central axis in order to provide the desired rotation at each blade. Whether the ring is translated or rotated, displacement of the point C causes pivots A and B to rotate, thus adjusting the IGV angle. The modified crank slider mechanism allows for more flexible actuation, both linear and rotational. This is achieved by replacing the pin joints in the mechanism with ball joints. This mechanism is more efficient and requires ~70% of the force the mechanism developed by Rusovici *et al.* 2011 required [10]. This mechanism required 2 N of linear force to actuate one vane at maximum load, which would require a total of 24 N for all twelve vanes. Thus, the entire new VIGV array could be actuated using three PI$^{TM}$ N310 piezo-inchworm actuators. Figures 10 (a&b) show the minimum and, respectively, the maximum deflection position.

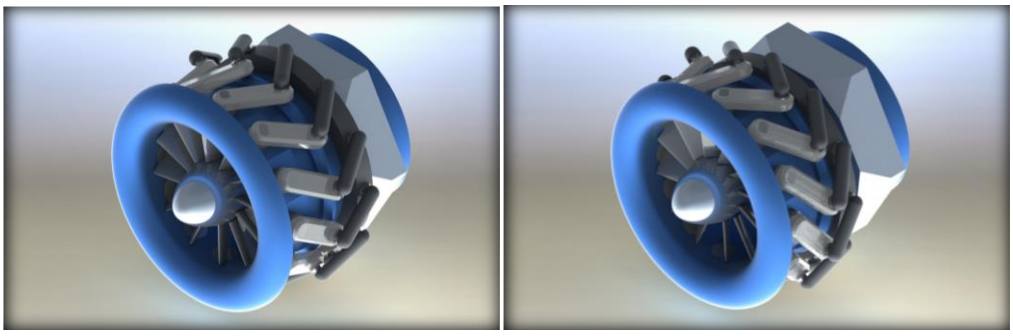

**Figure 10(a &b)** Linear configuration position 1(a) and 2(b)

### 2.1.1. Crank-slider displacement

The displacement of the crank slider mechanism was easily calculated using Equation 1. Figure 10 shows a horizontal crank-slider mechanism, where a horizontal displacement of point C to C' causes AB to rotate $10^0$. The displacement |CC'|, changes the positions of the links, which results in rotation of the IGV located at pivot point A.

$$|CC'| = 2 \cdot \cos(\theta) \cdot 25mm \quad \textbf{(1)}$$

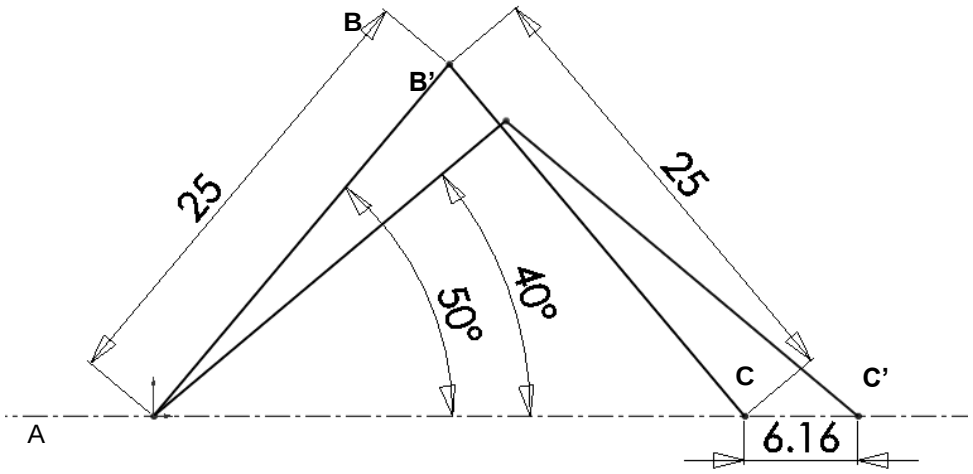


**Figure 11:** Sketch of the linkages with X axis slider, dimensions in mm

If both link |AB| and link |BC| were 25 mm long, the maximum projected linear displacement for a $10^0$ angular adjustment was determined to be 6.16 mm, which would be well within the capabilities of the piezo-inchworm actuator.

## 2.2 Piezo-inchworm actuator power considerations

The piezo-inchworm motor was selected as one of the possible actuators for the proposed VIGV mechanism. Precise positioning, relative fast response, large displacements (as compared to piezoceramic stack actuators) were all qualities that recommended the use of the piezo-inchworm.

The piezo-inchworm offered very precise control with a relatively large output force, good energy efficiency and overall lightweight construction. The piezomotor does not suffer from many parasitic mechanical losses, as there are very few moving parts associated with its movement. Moreover, the inchworm actuator would hardly consume any energy while holding its position, even while it would be withstanding a load up to 10 N. During this fixed position and force phase,the inchworm would be in a passive state (only the controller would be powered up), and no charge would be applied to either set of piezo stacks. It was noteworthy that while offering a considerable savings in power consumption, the piezomotor array can move the array at a maximum frequency of 2Hz. The piezo-actuator power calculations are shown in Equation 2. In Table 1, the maximum power $P_{max}$ required for piezo-inchworm actuation is presented and was found to be 1.8 W. The piezo-inchworm actuator had the following actuation parameters:

- Current constant (active): 0.25 A/N
- Current (passive): 0.45 [11]
- Nominal voltage: 0.4 V [11]

Equation set 2 provides the power calculations for the piezo-inchworm actuator.

$$A_{Max} = 0.20\frac{A}{N} \cdot 22.46\ N = 4.49\ A$$
$$P_{Max} = 5.62\ A\ \cdot 0.4\ V = 1.80\ W \quad \textbf{(2)}$$

**Table 1** Actuation power

| Drive | Piezo-inchworm |
|---|---|
| $P_{Max}$ Required (W) | 1.80 |

### 2.2 Piezo-inchworm actuator integration

The piezo-inchworm motor would be integrated in the linear mechanism. Three PI™ N310 Piezowalk motors by Physik Instrumente [11] would be arranged in an annular fashion on the outside of the engine casing. These actuators would bring a total force of well over 22.5 N, the required force for the mechanism to be actuated under the highest expected loads at a FS of 1.2. The N310 inchworm would be configured to be locked at rest, meaning that when the piezo array would not be powered, the actuator could still exert keep it position and maintain its maximum force of 10 N without any movement. These piezo-inchworm actuators offer a maximum travel of 10 mm. Figure 12 shows the position of these motors as integrated within the actuation mechanism.

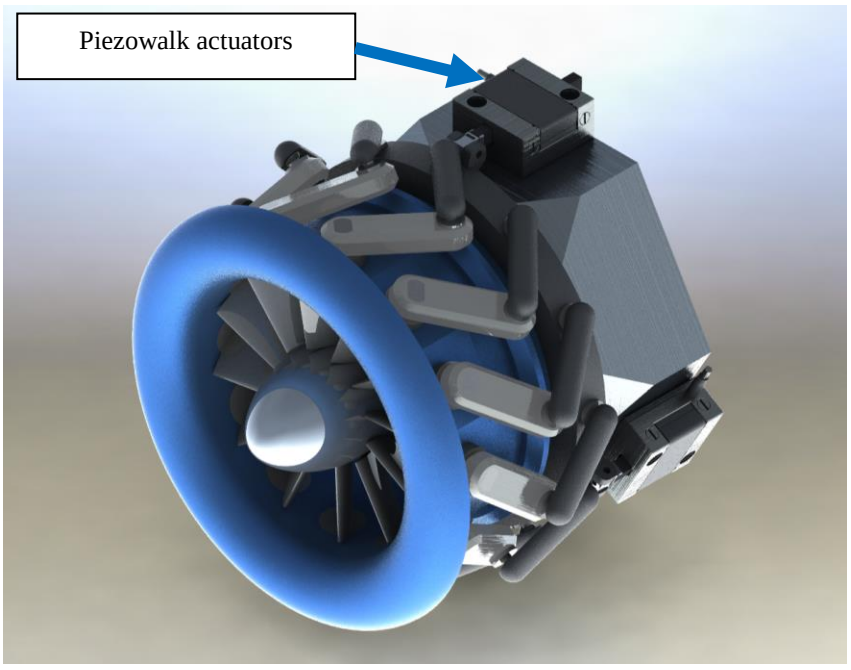


**Figure 12** Piezo-inchworm powered linear array

### 2.2 Mechanism design: structural considerations

The maximum displacement needed for each actuation mechanism was ~6.2 mm. Each IGV was subjected to a torque of 0.05 N-m due to the maximum aerodynamic loading. The Equation sets 2 and 3 outline the calculations

performed for the actuation force required per IGV. These calculations were based on simple mechanics of materials calculations presented in Beer *et al*. (2003), and on the free body diagrams (FBD) presented in Figures 13.

Figure 13 shows the FBD for the linear configuration of the mechanism. The resultant force Fc was broken up into its horizontal and vertical components, $F_{C(x)}$ and $F_{C(y)}$. This was done because the linear mechanism's actuators only needed to compensate for the horizontal component of the resultant force. Parameter θ represented the angle between the mechanism link and the horizontal.

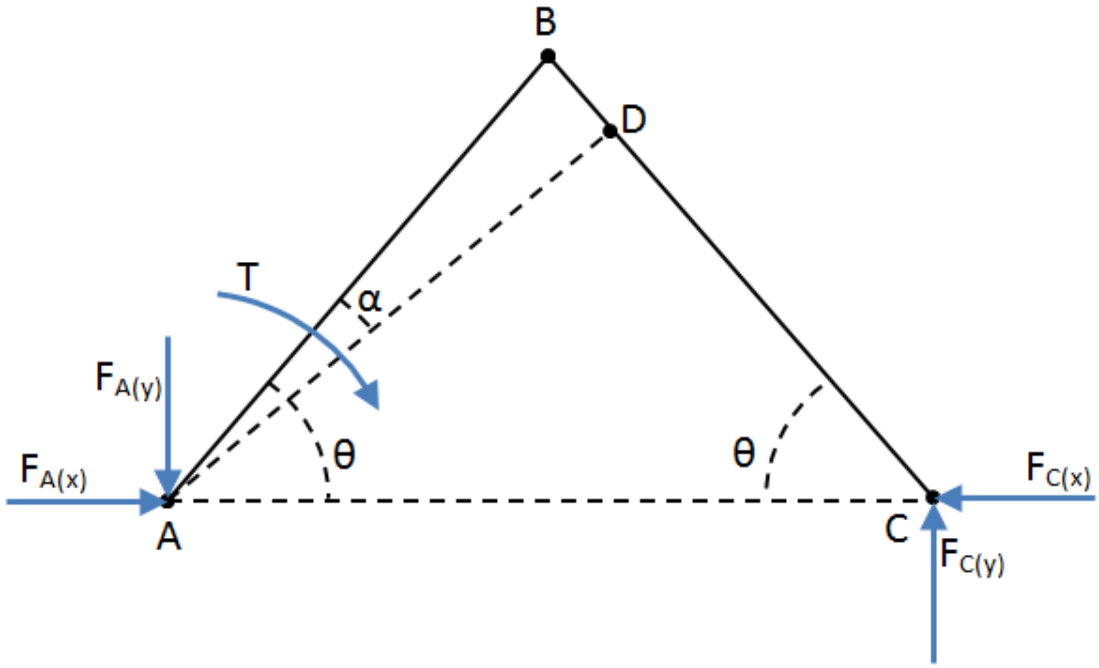


**Figure 13: Linear free body diagram**

Since distances AB and BC were equal to 25 mm, θ varied from 40° to 50°, and the resulting actuation moment was 0.05 N*m , derived from the aerodynamic loading on the blade, the following calculations led to the results in Figure 14.

$$\begin{aligned} \propto &= |90 - 2\theta| \\ |AD| &= \cos(\alpha) \cdot |AB| \\ F_{C(x)} &= \frac{T}{|AD|}\cos(\theta) \end{aligned} \quad \textbf{(3)}$$

A design of the crank-slider mechanism was performed using the force calculations in links and was aided by structural finite element analysis (ANSYS™) of the mechanism components. The model was constrained by applying a fixed condition at the attachment collar of the inlet guide vane. Then a frictionless support was added to the inside faces of the ring, thereby allowing it to translate strictly axially, with no secondary translation or rotation. Each mechanism was positioned in such a way that the IGV are fixed at their maximum angle of attack of $45^0$, while the actuator ring around the case applied maximum necessary force adjusted for a factor of safety of 1.5. This translated into a 1.87 N actuation force for each vane in the linear setup, and a 0.10 N*m torque for each vane in the rotary configuration.

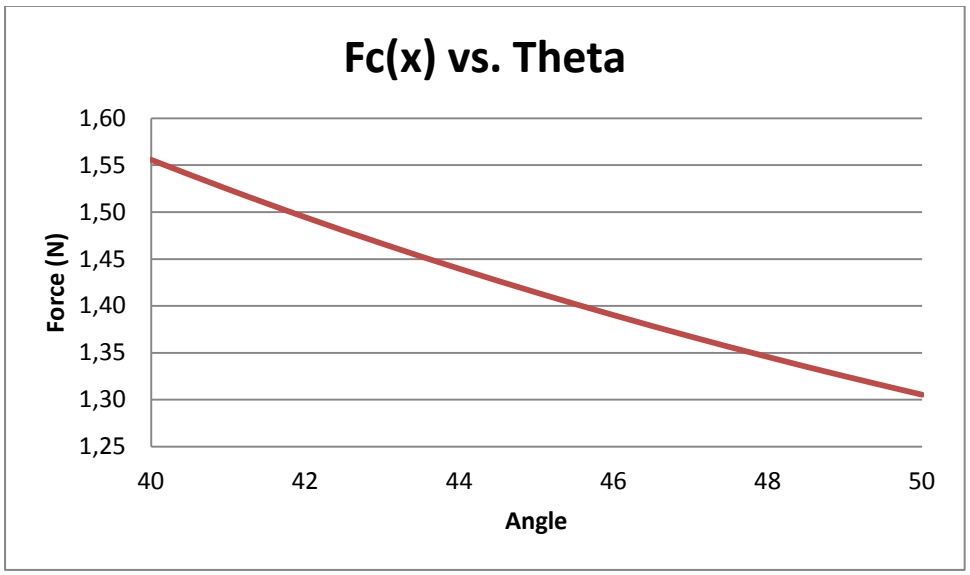


**Figure 14:** Force vs. linkage angle θ results

Thus, a total distributed force of 1.87 N was applied to the back face of the ring. The force distribution was non-uniform, but concentrated at the top, near the active linkage. This was done in an effort to reduce and binding due to misalignment of the ring with the case. The contact between the ball joint surfaces was set to frictionless as well. Figure 15 shows the boundary conditions and the model used. Most parts in the assembly were assumed to be made of aluminum 6061-T6, with the exception of 304 stainless steel for the ball joint pins and Nylon 6/10 for link BC and the mechanism ring. The stainless steel to polymer contact surfaces would provide minimal friction between these moving parts, while the polymer should still be more than strong enough to withstand the required forces

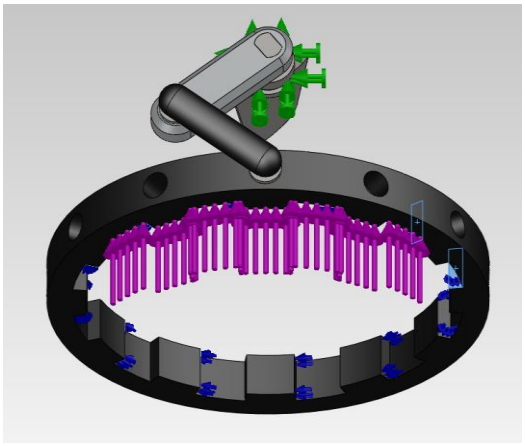

**Figure 15:** Sliding ring with one VIGV and mechanism

Figure 16 shows the Von Mises stress distribution in the mechanism, with one vane represented. Table 2 shows the simulation results.

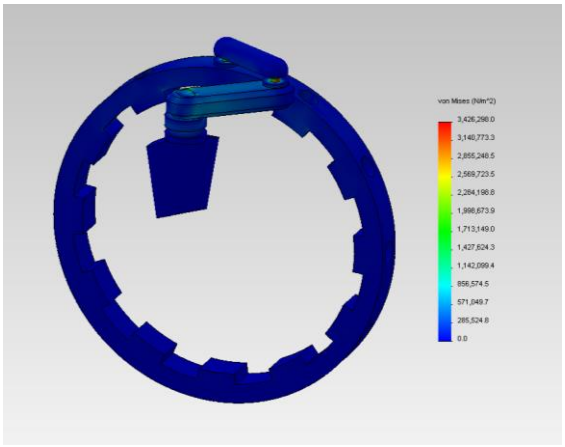


**Figure 16:** Von Mises stress distribution in linkage

**Table 2** Results for linear model FEA of mechanism

| | |
|---|---|
| Maximum stress | $3.4 \cdot 10^{6}$ Pa |
| Maximum displacement | $1.19 \cdot 10^{-2}$ mm |
| Minimum FS | 53 |

The results show that while the links were overdesigned, the conceptual design would work. While the parts could still be made significantly thinner in a future effort to reduce the overall weight of the mechanism, this would make the fabrication and assembly of the links and ball joints more cumbersome and expensive, as machining time to fabricate the links would increase significantly. The large factor of safety also allows the use of cheap materials such as aluminum 6061-T6 beyond its recommended temperature range, as opposed to a more expensive alloy that is more suitable to the temperature range of the turbine. The whole linkage assembly would weigh just 75 g in its current state of design, and further miniaturization of the components was not deemed necessary at this stage of the design (conceptual stage). In a final design iteration, a final prototype for mass production, would exhibit thinner, dog bone-shaped links could, that would be made via casting or injection molding (as opposed to machining).

## 3. CONCLUSIONS

This research documented an unconventional approach to actuation of a variable IGV array. A novel mechanism was designed, and which could accept different actuator types such as conventional DC motors, as well as smart-actuator alternatives such as piezo-electric motors, electro-rheologic actuators, and Shape Memory Alloy (SMA) actuators. A “smart” actuation method was chosen, as opposed to a more “classic” approach, one employing electric servomotors coupled with hydraulic actuation. Electric servomotors are, while powerful and precise, not very efficient. Hydraulic actuation is not realistically feasible on the small scale characteristic of small turbine engines, because of a large head loss across small hydraulic lines. The necessary IGV actuation parameters were found from a numerical study, which considered an analytical solution to an incompressible, viscous flow through a linear vane cascade [10].

The primary goal of this project was to create a conceptual design of a realistic mechanism for a VIGV system designed for small turbojet engines. VIGV offer significant performance benefits in specific flight regimes, and have been used on large turbine engines for over 60 years. The mechanism design used in this paper is based on a simplified GE 79-style reverse crank slider mechanism. The mechanism was designed to performance parameters

given by an existing small-scale, jet engine. In order to actuate the mechanism successfully, the aerodynamic load onto each inlet guide vane was considered and the necessary output force for the actuators was calculated. Many 'smart' actuator alternatives promise compromise-free operation, but in reality many of them are still either impractical to use in a small UAV, or cannot achieve the necessary output requirements. After careful consideration and comparison, the PI™ PiezoWalk linear actuator was selected. The piezo-inchworm motors offer a significant advantage over the DC motors in the fact that they can withstand the maximum loads of the mechanism without being powered on, while the DC motors have draw a constant current, even when no movement of the array is necessary.

In conclusion, the conceptual design approach described here was successful. A piezoelectric inchworm actuation system was designed for a VIGV array in a small turbojet, one that could provide the required performance requirements and prove to be more efficient than a conventional power system for the mechanism.

## REFERENCES

1. Freed, M., Harris, R.; Shafto, M. G. , "Human-interaction challenges in UAV-based autonomous surveillance ", AAAI Spring Symposium Interaction between Humans and Autonomous Systems over Extended Operation - Technical Report, Vol. 3, 2004, pp. 65-70.
2. Bailie, S. T., Ng, W. F., Copenhaver, W. W., "Experimental reduction of transonic fan forced response by IGV flow control", Proceedings of the ASME Turbo Expo 2004, 2004, Vol. 6, pp. 527-537.
3. Rodgers, C.,"Centrifugal compressor inlet guide vanes for increased surge margin", American Society of Mechanical Engineers (Paper), GT158 7p, International Gas Turbine and Aeroengine Congress and Exposition, June 11-14, 1990.
4. Hill, P., Peterson, C.,"Mechanics and Thermodynamics of Propulsion" Second Edition, Prentice Hall, Upper Saddle River, New Jersey 1992.
5. Wanger, Robert. "Duct with vanes having selectively variable pitch." United States Patent, Patent Number 3,861,822. 1974.
6. Patel, Manubhai, "Variable inlet guide vanes for an axialflow compressor" United States Patent, Patent Number 4,950,129 (989.
7. Hartman, A.W., "Piezoelectric inchworm operation in a vacuum", Optical Engineering, Vol. 17, No. 6, Nov-Dec .1978, pp. 645-646
8. Lobontiu, N. ,Goldfarb, M., Garcia, E., "Piezoelectric-driven inchworm locomotion device", Mechanism and Machine Theory, Vol. 36, No. 4, April 2001, pp. 425-443.
9. Emery, J.C., Herrig, J. L., Erwin, J. R., Felix, A. R., 1958, "Systematic two-dimensional cascade tests of NACA 65 series compressor blades at low speeds", NACA Report 1368, 1958.
10. Rusovici, R., Sepri, P., Feys, J., Kwokchoon, S., "Smart actuation of inlet guide vanes for small turbine engines", Sensors and Smart Structures Technologies for Civil, Mechanical, and Aerospace Systems, SPIE Proceedings 7981, April 2011.
11. Physik Instrumente, Products Catalog, 2012.